INVITED PAPER   *Special Section on Microwave and Millimeter-Wave Technologies*

Link Design and Techniques of Microwave Power Transfer for Latest Power Utilization Systems on Beyond-5G/6G

Naoki HASEGAWA[†a)], *Member*

SUMMARY   The expansion of the communication area is expected for Beyond-5G/6G networks using the High Altitude Platform Station (HAPS), Internet of Things (IoT), and sensor devices. Beyond-5G/6G networks constitute the vast amounts of devices that require the latest power utilization system. We expect Microwave Power Transfer (MPT) plays a role in the wireless power supply to HAPS, IoT, and sensors in this network. This work discusses the link design and techniques of MPT for the newest power utilization system required on Beyond-5G/6G networks.
key words: *Microwave Power Transfer, Beyond 5G/6G, Magnetron, simple beamformer*

1. Introduction

Microwave Power Transfer (MPT) is planned to be used in next-generation power utilization systems for wireless energy supply. High Altitude Platform Station (HAPS), drones, and Internet of Things (IoT) are likely to be employed for Beyond 5G/6G communications. Furthermore, sensor network systems are required to bring society 5.0 where cyberspace and physical are fused by digital transformation techniques. In addition, the use of HAPS and drone base stations are expected to expand the area of data communications services. These flying base stations require a constant power supply. MPT is an effective method for powering drones or HAPS in flight.

MPT techniques have been previously discussed and reported. In 1964 Brown reported an MPT demonstration for a flying helicopter [1]. Brown also demonstrated 30 kW power transfer within a 1.54 km distance using a large parabolic antenna in 1975 [1]. Moreover, a Stationary High Altitude Relay Platform (SHARP) was proposed in Canada in 1980 [2]. The SHARP was designed to provide 500 kW of electricity to an unmanned airplane in the stratosphere. In Japan, a MIcrowave Lifted Airplane eXperiment (MILAX) was tested in 1992 [3]. In the MILAX demonstration using a 4 kg unmanned airplane, 1.25 kW of electricity was transferred at 2.411 GHz at an altitude of 10 m. In 1995, Energy Transmission to a High Altitude Long endurance airship ExpeRient (ETHER) was demonstrated in Japan [4]. In the ETHER experiment, 10 kW of power was transferred at 2.45 GHz at a 45 m altitude utilizing a 16 m blimp. The beam-type wireless power transfer

(WPT), including MPT, was intended to be used for wireless power charging of mobile or wearable devices, sensors, and IoT. The establishment of beam-WPT has been discussed on ITU-R since 2013 [5].

MPT systems for the next-generation power utilization systems should be built around large-aperture antennas. Additionally, MPT system configurations for HAPS have been previously reported and discussed. The SHARP projects assumed an 80 m diameter Tx antenna for MPT to an airplane at 20 km altitude at 5.8 GHz [2]. In [2], the large-scale rectenna array with 86 cm diameter was demonstrated. A large-aperture antenna also helps increase antenna gain, improving the power transmission efficiency. It is possible to use a phased array technique for beamforming in the MPT system. Generally, many studies on phased array antennas for MPT have been published [6]–[11]. In [6], a 5.8 GHz phased array antenna with 256 elements was created. Ishikawa et al. reported flat-topped beamforming based on the phased array antenna established in the experiment for MPT to electric vehicles [7]. In conventional research reported by the author, a technique for side-lobe reduction based on tuning GaN amplifiers was demonstrated [8]. In addition, when it comes to MPT for IoT or sensors, a large-aperture antenna system based on the phased array antenna is beneficial for high-efficiency power transmission. The beamforming technique based on the phased array antenna helps the MPT system for IoT or sensors that require multitargeting and tracking for many devices.

The MPT system enables the distribution of HAPS, drone, IoT, and sensor networks over Beyond-5G/6G networks and society 5.0. In Japan, the institution for the MPT system at 920 MHz, 2.4 GHz, and 5.7 GHz has already been discussed. However, the transmission efficiency of these MPT systems at the sub-6 frequency is based on a few assumptions. The sub-6 frequency band is home to 99.98% of all radio stations. Therefore, it is critical to discuss optimal frequencies. Improving efficiency is also essential for achieving social goals. In this paper, we first discuss the link design of MPT systems for HAPS and IoT. During this discussion, we determined an appropriate frequency for each application. Next, we introduce the crucial techniques for MPT to HAPS or IoT.
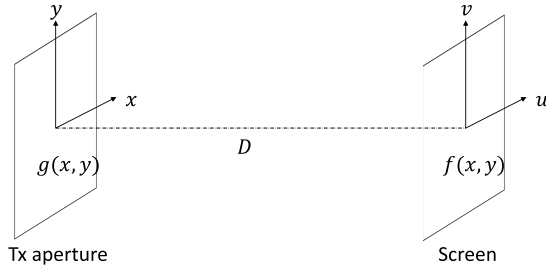
Fig. 1 The coordinate system for calculating the microwave propagation using Fresnel diffraction.

Fig. 2 State-of-the-art rectifier efficiency.

2. Link Calculation Methods

2.1 Microwave Propagation

Friis transmission formulas are commonly used in wireless system propagation design. However, the Friis transmission formula is a calculation method assuming a Fraunhofer distance and cannot be used for Fresnel distances. A method of deriving the received electric field distribution from the Fresnel diffraction equation is utilized to compute the link budget at a Fresnel distance. In this equation, the electromagnetic field on the receiver aperture is calculated using the source wave interference on the transmission aperture. The electric field distribution f on the receiver aperture is calculated employing the following equation based on the coordinate system as shown in Fig. 1;

$$f(u,v) = A' \int \int g(x,y) e^{j\frac{k}{2D}(x^2+y^2)} e^{-j\frac{k}{D}(ux+vy)} dx dy, \quad (1)$$

$$A' = \frac{1}{j\lambda D} e^{jk(D+\frac{u^2+v^2}{2D})}, \quad (2)$$

where $g(x,y)$ is the electric field on the transmission aperture, λ is the wavelength, k is the wave number, and D is the distance between the transmission and receiving antennas.

The antenna size causes a path difference in the Fresnel, leading to a phase difference on the Rx antenna surface. This phase difference provides an efficiency reduction. As a result, we assume focused beam tuning of the phase distribution on the Tx antenna aperture to compensate for the path difference. In the focused beam, the phase distribution $\arg g(x,y)$ on the Tx aperture is given by the following equation;

$$\arg g(x,y) \simeq -\frac{k}{2D}(x^2 + y^2). \quad (3)$$

2.2 Rainfall Attenuation

Rainfall generally affects microwave propagation. Thus, it is crucial to understand the impact of rainfall on link budgets in MPT systems. The model of rain attenuation γ per 1 km is standardized by ITU-R [12]–[14] via the following equation;
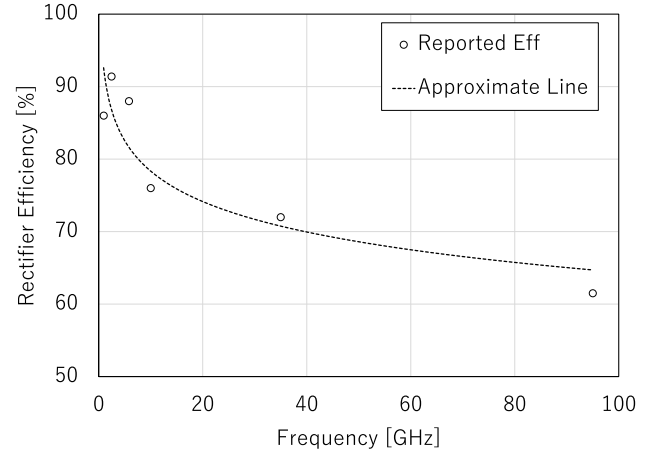
$$\gamma = kR^{\alpha} \quad (4)$$

$$\alpha = \sum_{j=1}^{5}\left(a_j \exp\left[-\left(\frac{\log_{10} f - b_j}{c_j}\right)^2\right]\right) + m_{\alpha} \log_{10} f + c_{\alpha}, \quad (5)$$

where f is frequency, k is wave number, and R is rain rate per hour. Furthermore, a_j, b_j, c_j, m_k, and c_k are dependent on the path elevation angle and polarization tilt angles are provided as the constant values in [12].

2.3 Rectifier Efficiency

The rectifier is a core technology for the MPT system. The high-efficiency rectifiers have been previously discussed and reported. The RF-to-DC efficiency of state-of-the-art rectifier reported in [15]–[20] is plotted in Fig. 2. According to Fig. 2, the efficiency logarithmically decreases with increasing frequency. The rectifier efficiency is approximated by a logarithmic curve and incorporated into the line design. The following equation represents the approximate curve;

$$\eta_{\text{rec}} = -0.06 \ln f + 0.92, \quad (6)$$

where η_{rec} is the rectifier efficiency, and f is the frequency.

3. Target Applications and Models

3.1 HAPS

The HAPS is expected to expand the area of mobile communications and environmental observations. At an altitude of about 20 km, the stratosphere has more stable weather than the troposphere, making it suitable for a fixed-point flight of unmanned flying objects.

In this link calculation, we assume a system model as shown in Fig. 3 and rectangular Tx and Rx antenna aperture with an area of 5674 and 0.58 m^2, which are the same antenna square measurements as in the SHARP [2]. We also assume that the antennas face each other for simplicity. The
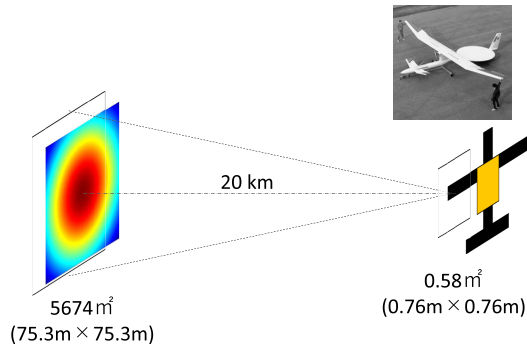
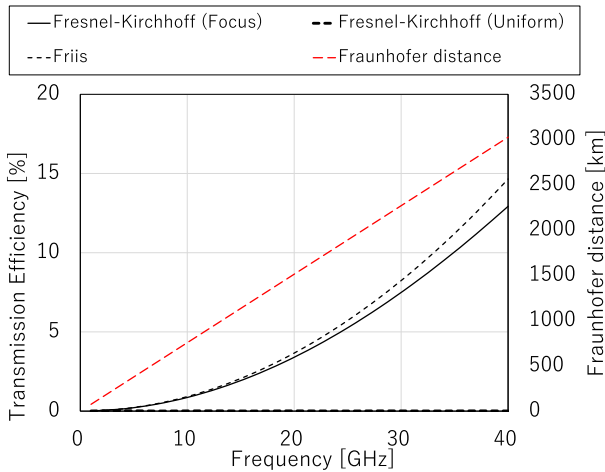**Fig. 3** MPT system model for HAPS on 20 km stratosphere.

Fig. 4 The calculated transmission efficiency based on Friis and Fresnel equations and fraunhofer distance for MPT system to HAPS.

Fig. 5 Rain attenuation on the MPT system for HAPS.

Fig. 6 Transmission efficiency calculated using the focus beam based on the Fresnel diffraction equation with rainfall attenuation.

calculated transmission efficiency and boundary to a Fraunhofer distance from a Fresnel distance are shown in Fig. 4. The Fraunhofer distance, calculated as $2D/\lambda^2$, is the boundary between the Fraunhofer and Fresnel distances. According to Fig. 4, the Friis equation is split with Fresnel to provide a uniform phase distribution for the Tx antenna aperture. This gap widens with increasing frequency. According to the Fraunhofer distance, the antenna size provides Fresnel propagation in this frequency band, contributing to the overestimation of the Friis equation result. In the focused beam, the phase difference distribution on the Tx antenna aperture is tuned, enhancing the transmission efficiency at a Fresnel distance. Consequently, the result based on Fresnel with focus beam tuning is improved, which matches the results based on the Friis equation. This result exhibits the effectiveness of focused beams for MPT systems in HAPS.

The rainfall affects the long-rang MPT to HAPS by attenuating microwave propagation. Furthermore, rainfall attenuation can be calculated by (4). For the sake of simplicity, we assume that the path elevation and polarization tilt angles are both zero. Additionally, we calculated the propagation assuming a 10 km microwave attenuation section because rainfall generally exists in the troposphere up to about 10 km in altitude. The standard values for heavy
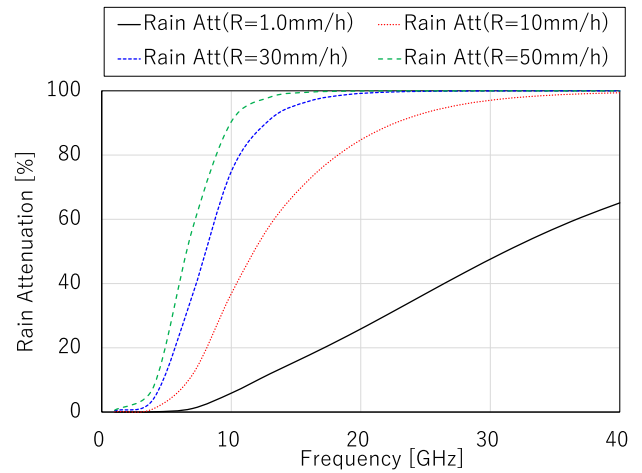
rain warnings are approximately 10 to 50 mm/h. The calculation results of the attenuation based on rainfall with 1.0, 10, 30, and 50 mm/h for MPT to HAPS are illustrated in Fig. 5. According to Fig. 5, we found that heavy rain has an effect on microwave propagation at higher frequencies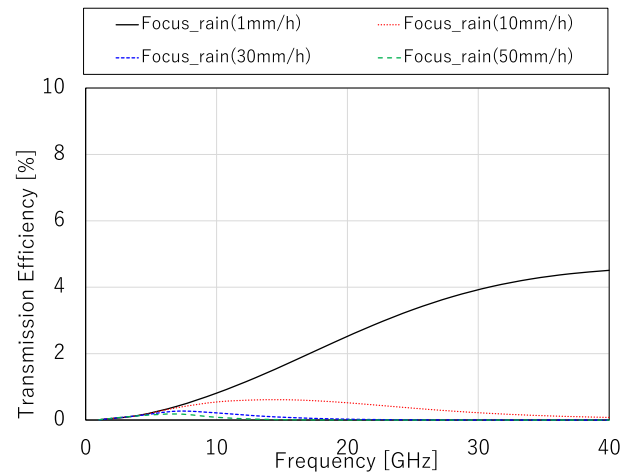. The transmission efficiency calculated using focused beams based on the Fresnel diffraction equation with rainfall attenuation is shown in Fig. 6. According to Fig. 6, the transmission efficiency degradation for each rainfall rate increases with rainfall attenuation at high frequencies. Even if it is negatively influenced by 1.0 mm/h rainfall, the MPT with high frequency has higher efficiency compared to the sub-6 mm-wave frequency range. However, microwaves cannot propagate in the mm-wave frequency range at speeds greater than 10 mm/h. Figure 7 depicts transmission efficiency by incorporating the rectifier efficiency from Fig. 2 into Fig. 6. According to Fig. 7, the transmission efficiency at the mm-wave frequency is also hugely attenuated compared to sub-6 frequency.
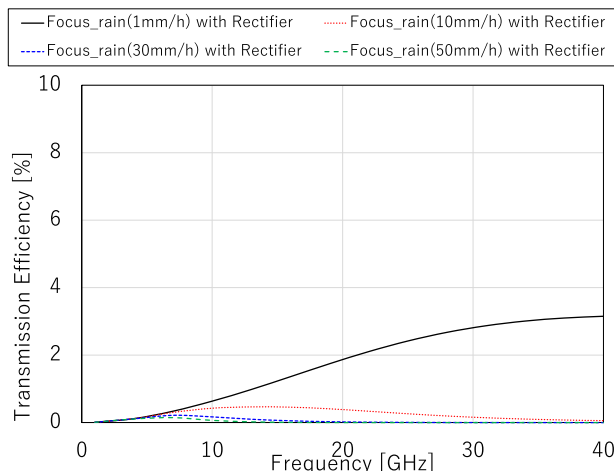
The received power on the MPT system for the HAPS

Fig. 7 Transmission efficiency computed utilizing the focus beam based on the Fresnel diffraction equation with rainfall attenuation and rectifier efficiency.

Table 1 Received power at 500 kW transmission for HAPS.

Freq.	1 mm/h	10 mm/h	30 mm/h	50 mm/h
2.4 GHz	0.21 kW	0.21 kW	0.21 kW	0.21 kW
5.7 GHz	1.18 kW	1.12 kW	0.96 kW	0.79 kW
24 GHz	11.75 kW	1.43 kW	0.04 kW	0.001 kW

at 2.4, 5.7, and 24 GHz is listed in Table 1. Moreover, 2.4, 5.7, and 24 GHz are the ISM frequency bands discussed for application in the MPT system in the ITU-R or many consortiums. In this calculation, we assume 500 kW power transmission as proposed on SHARP projects [2]. The transmission efficiency, rainfall attenuation, and rectifier efficacy are based on received power. This calculation does not consider that DC power combined from each rectifier is not included in this computation. It should also be noted that the calculation excludes the deterioration of propagation characteristics due to turning flight. This calculation clarified the critical conclusions of determining the appropriate frequency and developing MPT operation rules for rainfall. According to Table 1, the greater received power is obtained with up to 10 mm/h of rainfall in the MPT system based on 24 GHz RF propagation compared to 2.4 and 5.7 GHz. However, the received power significantly decreased above 10 mm/h rainfall. This result indicates the need for a system that restricts MPT operation for rainfall of up to 10 mm/h. According to [21], the mission allowable electric power for an unmanned solar plane such as Helios and Pathfinder Plus (Aero Viroment Inc.) is up to 1 kW. We confirmed that the calculated received power for up to 10 mm/h rainfall at 24 GHz meets the allowable mission electric power requirements.

3.2 IoT

IoT businesses are continually growing, and their numbers are expected to surpass one trillion by 2030. Furthermore,
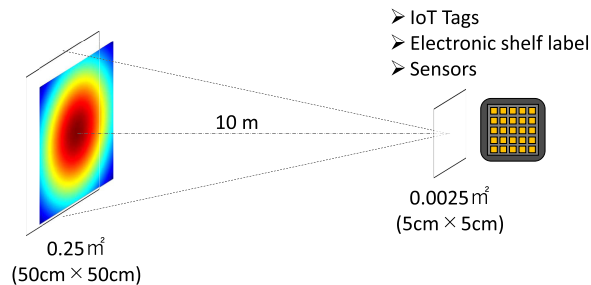

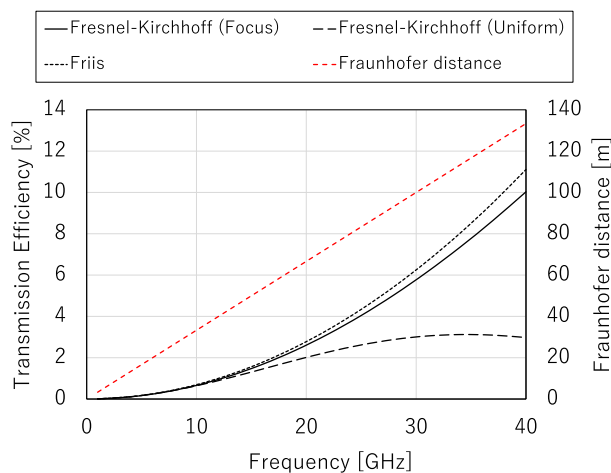**Fig. 8** MPT system model for IoT up to 10 m distance.

Fig. 9 The calculated transmission efficiency based on Friis and Fresnel-Kirchhoff equations and Fraunhofer distance for MPT system to IoT

high-sensitivity digital twin systems comprising massive sensors for an epochal society are projected. Our society must address the issue of power supply for massive devices. MPT systems are a critical technology for supplying several devices. In this paper, we introduce the microwave propagation calculation to the IoT or sensor antennas.

Figure 8 displays the MPT system model at a 10 m distance, assuming the application of a 50 cm × 50 cm Tx antenna and targeting a device with a size of 5 cm × 5 cm. Assuming that the aperture efficiency is 100-%, the antenna gain is calculated utilizing $4\pi S/\lambda^2$ where S is the antenna size, and λ is the wavelength. As a result, the antenna gains of 43.0 and 23.0 dBi at 24 GHz frequency are obtained for antenna sizes of 50 cm × 50 cm and 5 cm × 5 cm, respectively. In this calculation, we tune the phase distribution on the Tx antenna aperture to provide the focused beam. The calculated results, including the Fraunhofer distance, are illustrated in Fig. 9. Since these results are primarily calculated in Fresnel conditions, the Friis equation is split with Fresnel to provide uniform phase distribution for the Tx antenna aperture (see Fig. 9). On the other hand, the calculated result based on the focused beam improves the transmission efficiency and approaches the Friis formula.

Figure 10 presents the rain attenuation calculated using (4), assuming propagation for 10 m. According to these findings, rainfall has little effect on microwave propagation.
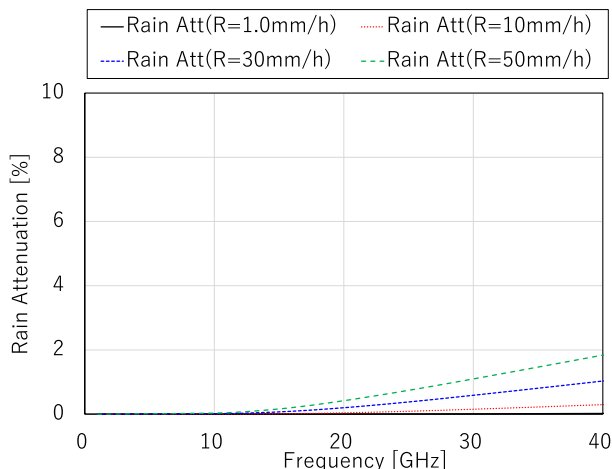
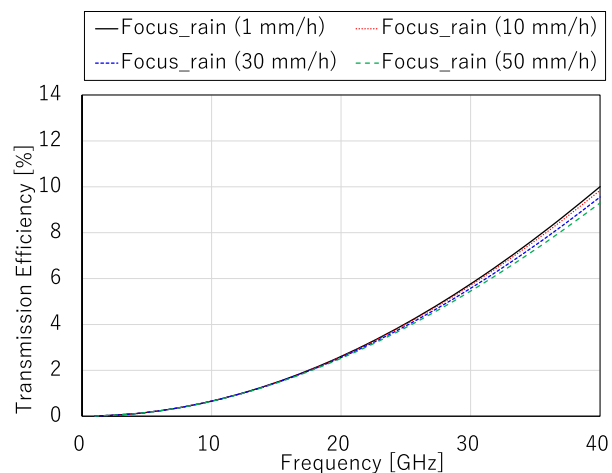**Fig. 10** Rain attenuation on the MPT system for IoT at 10 m distance.

Fig. 11 Transmission efficiency employing focused beam based on Fresnel diffraction equation with rainfall attenuation.

Fig. 12 Transmission efficiency calculated using focused beam based on Fresnel diffraction equation with rainfall attenuation and rectifier efficiency.

Table 2 Received power at 1 W transmission for IoT or sensors.

Freq.	1 mm/h	10 mm/h	30 mm/h	50 mm/h
2.4 GHz	0.33 mW	0.33 mW	0.33 kW	0.33 mW
5.7 GHz	1.75 mW	1.75 mW	1.75 mW	1.75 mW
24 GHz	27.25 mW	27.05 mW	26.59 mW	26.14 mW

Table 2 lists the received power on the MPT system for the IoT or sensors with a 5 cm × 5 cm antenna aperture at 2.4, 5.7, and 24 GHz. The transmission efficiency, rainfall attenuation, and rectifier efficacy are based on the received power. This calculation does not consider the DC power combining from each rectifier. According to Table 2, we confirmed that the MPT based on a 24 GHz frequency transmits more power to the target compared to 2.4 and 5.7 GHz. Rainfall has little effect on received power in each frequency band. We confirmed that we would receive enough power to run the IoT devices requiring a few mW of power, such as tags, electronic shelf labels, and sensors.

4. Key Techniques

The conclusions in the previous section signify that the transmission efficiency at higher frequencies is enhanced compared to the sub-6 frequency. However, the calculation was based on the necessity of a large-aperture antenna and beamforming such as a focused beam. The high-efficiency MPT requires the large-aperture beamformer based on a phased array antenna.

Figure 13 shows the configuration of the large-aperture beamformer. The output phases of each antenna are tuned in this configuration, which provides beamforming functions for target tracking and focused beamforming. Given that the MPT for HAPS requires a 5674-m^2 antenna aperture, it is feasible to use a parabolic array for antenna units. The antenna units are beam steered via mechanical driving such as gimbals. Furthermore, the phase variance between an-

This conclusion is supported by Fig. 11, depicting the transmission efficiency calculated using a focused beam based on Fresnel diffraction with rainfall attenuation.

The transmission efficiency in Fig. 12 calculated by using a focused beam based on the Fresnel diffraction equation with rainfall attenuation and rectifier efficiency is shown in Fig. 2. Additionally, the approximate curve (6) based on the state-of-the-art rectifier reports is used in this calculation. According to Fig. 12, we confirmed that the rectifier efficiency reduction at high frequencies slightly decreases the transmission efficiency.

In 2016, the Federal Communication Commission (FCC) decided that the maximum Equivalent Isotropically Radiated Power (EIRP) from a base station for 5G is 75 dBm/100 MHz [22]. In this link design, the received power is calculated using a reference value of up to 75 dBm EIRP. We assumed using a 44.37 dBi Tx antenna with a 50 cm × 50 cm aperture to calculate transmission efficiency. As a result, we assume a 1 W power transmission in this link design, providing the 74.37-dBm EIRP for the Tx antenna.
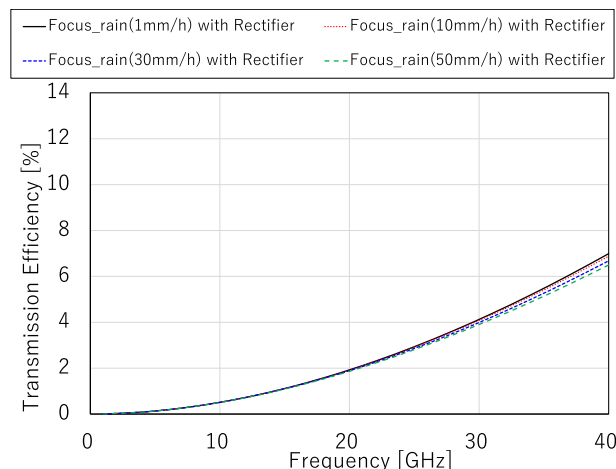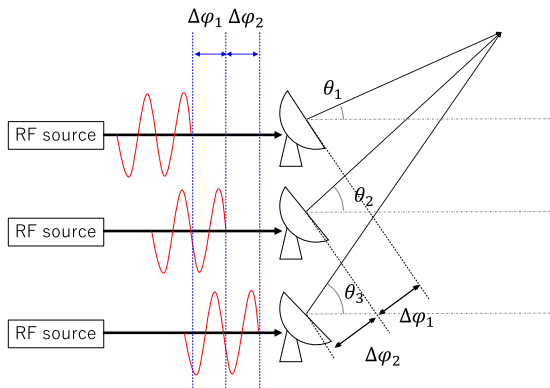
Fig. 13 The configuration of large-aperture beam former.

Fig. 14 Magnetron transmitter with injection locking for output phase tuning.

tenna units due to the path difference should be tuned on the RF sources. Conversely, replacing the antenna parabolic units with phased array antenna units is useful, considering the MPT for IoT or sensors. The phased array technique is widely used in massive-MIMO data communication. For MPT, beamforming based on the phased array technique has been discussed [23]–[28]. In this section, we discuss the key techniques for configuring the antenna system depicted in Fig. 13.

4.1 High-Power Transmitter

For the MPT system to HAPS, a high-power transmitter is required. High-power vacuum oscillators are widely used, such as Klystron, Gyrotron, and Magnetron. The Klystron and Gyroton, which are used in many fields such as radar, communication, and plasma, can operate above the Ka-band frequency. Alternatively, Magnetrons above 1 kW are widely used up to the C-band frequency, which is expected to be an inexpensive RF source. Magnetrons are used in microwave ovens and are cost-effective, high-power RF sources. However, the Magnetron output signal is generally unstable, resulting in a broad frequency spectrum. In this section, taking the Magnetron as an example, the output phase control method of the transmitter using the injection-synchronization phenomenon is explained.

Recently, an MPT system based on phase tuning Magnetron techniques was proposed [29]–[33]. The output signal of a phase-locked Magnetron is synchronized by an injected signal, allowing for high spectral purity and accurate phase control of the transmitter. Phase tuning Magnetron based on injection locking technique was reported in our research [34]. The two-way Magnetron transmitter was used for the demonstration, as shown in Fig. 14. In this demonstration, 1 kW Magnetron units (M5803, Panasonic) operated at 5.8 GHz were used. An RF signal for phase tuning is injected into the Magnetrons through a circulator in this configuration, which provides output phase locking. Figure 15 depicts the measured output spectrum of a Magnetron, including and excluding injection locking. According to Fig. 15, the RF signal for injection locking im-
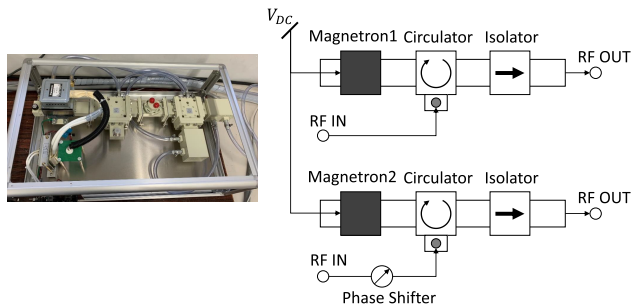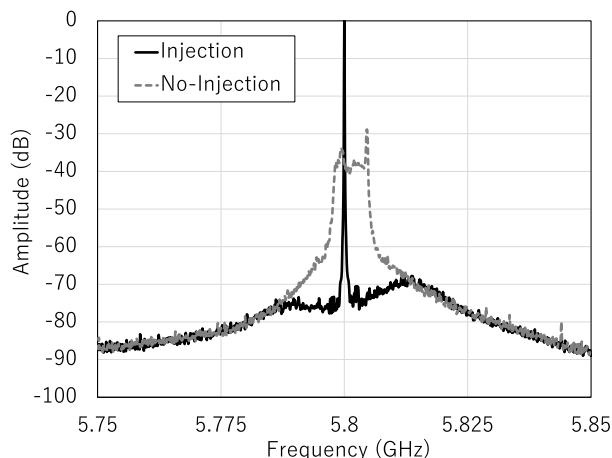

Fig. 15 Measured output spectrum from the Magnetron including and excluding injection locking.
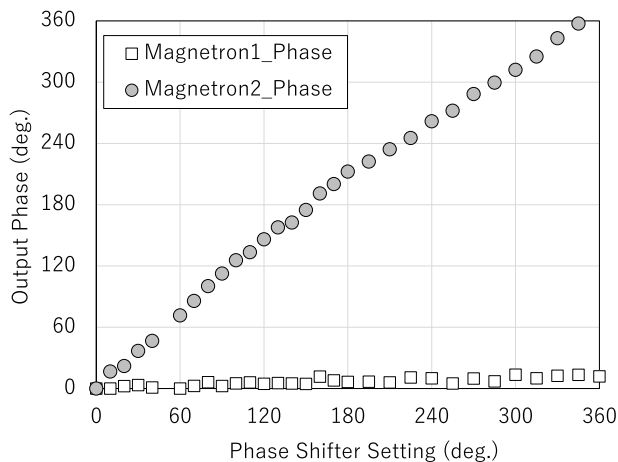

Fig. 16 Measured output phase from the phase tuning Magnetrons.

proves the broad spectrum and provides the narrowband output spectrum. Figure 16 illustrates the output spectrums of each Magnetron. According to Fig. 16, the measured output phase from "Magnetron2" tuned by the input phase follows the value of the phase shifter setting proportionally.
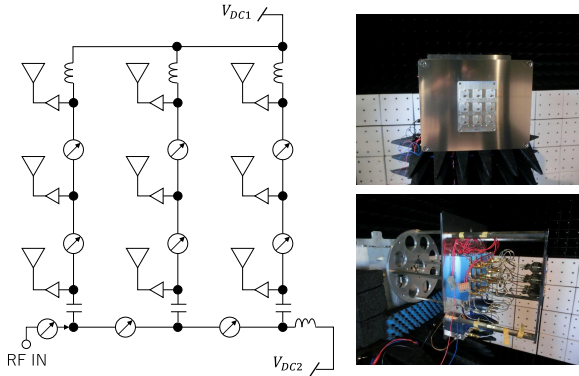
Fig. 17 Antenna configuration for simple beam steering based on traveling-wave feeding.

Fig. 18 The conflation of large-aperture beam former based on the traveling-wave antenna units.

4.2 Simple Beam Former

The beamforming technique based on the phased array antenna has been used in numerous fields such as radar, mobile communication, and MPT. In wireless systems, digital beamforming is widely used on MIMO systems such as 5G communication. Moreover, RFIDs are used to tune the amplitude and phase of each antenna element in the full-digital beamforming system. The RFIDs generally consist of RF circuits such as a phase shifter, amplifier, and mixer. The full-digital beamformer requires as many RFICs as the antenna element, meaning that the same amount of RFICs is necessary for this beamformer and phase control system as the conventional parallel-fed array antenna.

The required antenna elements are increased to 6400 elements at 24 GHz, assuming a 0.5 λ antenna pitch and considering the Tx antenna with an aperture of 50 cm × 50 cm for MPT to IoT or sensors, as shown in Fig. 8. Designing a simple and reasonable antenna system in the conventional phased array is challenging when attaching the RFIC to each antenna element. In our research, we proposed a technique based on traveling-wave feeding [35].

The antenna configuration for simple beam steering based on traveling-wave feeding is illustrated in Fig. 17. The beam angle in this configuration is dependent on the phase difference between adjacent antenna elements. Moreover, the two-way DC bias of V_{DC1} and V_{DC2} provides the two-dimensional (2D) beam steering, assuming the output phase from the phase shifters tuned by a DC bias voltage. Figure 18 presents the conflation of large-aperture beamformer based on the traveling-wave antenna units. The 2D traveling-wave antennas are used for the antenna units instead of the parabolic antennas, as shown in Fig. 13. We obtained the measured radiation patterns at 5.8 GHz frequency (see Fig. 19 and Fig. 20) using the traveling-wave antenna, as shown in Fig. 17. According to Fig. 19 and Fig. 20, we confirmed the 2D beam steering by only tuning V_{DC1} and V_{DC2}.
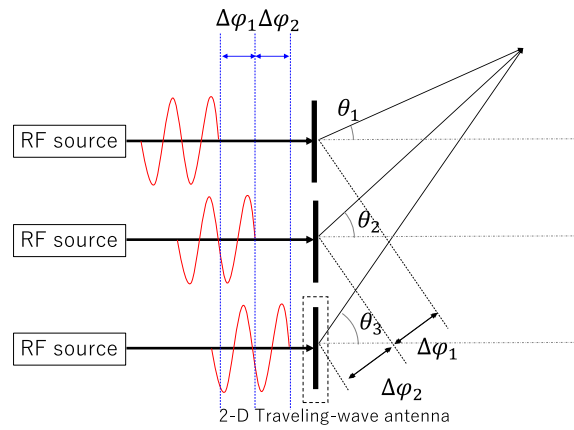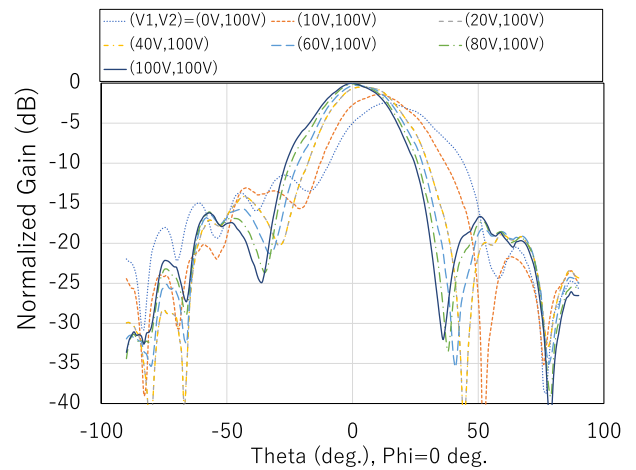

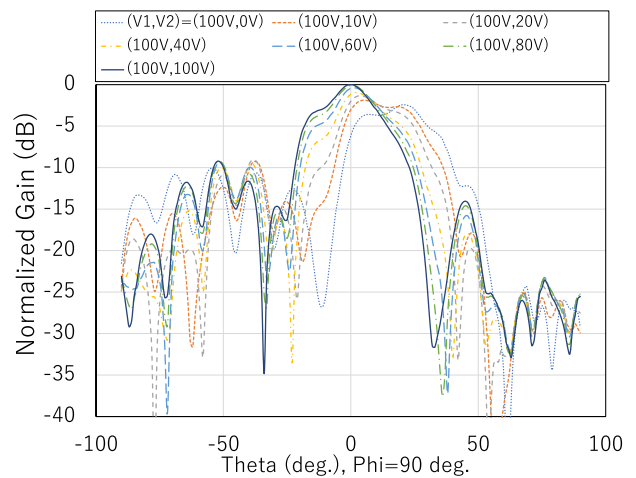**Fig. 19** Measured radiation patterns on phi = 0 ° axis when tuning the V_{DC1}.

Fig. 20 Measured radiation patterns on phi = 90 ° axis when tuning the V_{DC2}.

5. Conclusion

The expansion of the communication area using HAPS is expected in Beyond 5G/6G networks. Furthermore, power supply to IoT or sensors is required for using an expanded function for Beyond 5G/6G network-based station. As a result, we anticipate that the MPT will supply wireless power to HAPS, IoT, and sensors in Beyond-5G/6G networks for the most current power utilization system.

The link design of MPT systems for targeting HAPS and IoT was discussed using simple transmission models. Rainfall attenuation and rectifier efficiency were included in these models. We confirmed the calculated received power up to 10 mm/h rainfall at 24 GHz satisfies the mission allowable electric power, assuming transfer for a HAPS at a 20 km altitude. Furthermore, we received sufficient power for running the IoT devices, such as tags, electronic shelf labels, and sensors requiring a few mW of power. These results are calculated with the Tx and Rx antennas facing each other, and the effect of the antenna's position and orientation is still in question.

Furthermore, this paper introduced the key technologies for constructing a large-scale antenna aperture for MPT systems for HAPS and IoT. The antenna array system with phase tuning based on the injection-lock Magnetron was introduced in the MPT system for HAPS requiring a high-power transmitter. On the other hand, a simple beamformer based on traveling-wave feeding for the MPT system to IoT or sensor was introduced. These techniques were applied to build a simple and reasonable antenna system, significantly reducing social implementation challenges.

Acknowledgments

References

[1] W.C. Brown, "The History of Power Transmission by Radio Waves," IEEE Trans. Microw. Theory Tech., vol.32, no.9, pp.1230–1242, Sept. 1984.

[2] J.J. Schlesak, A. Alden, and T. Ohno, "A microwave powered high altitude platform," in Proc. IEEE MTT-S Int. Microw. Symp., New York, NY, USA, vol.1, pp.283–286, 1988.

[3] H. Matsumoto, N. Kaya, M. Fujita, Y. Fujino, T. Fujiwara, and T. Sato, "MILAX airplane experiment and model airplane," in Proc. 11th ISAS Space Energy Symp., pp.47–52, 1993.

[4] N. Kaya, S. Ida, Y. Fujino, and M. FUjita, "Transmitting Antenna System for Airship Demonstration (ETHER)," Space Energy Transportation, vol.1, pp.237–245, 1996.

[5] ITU-R: Report ITU-R SM.2303-2, "Wireless power transmission using technologies other than radio frequency beam," 2017.

[6] Y. Homma, T. Sasaki, K. Namura, F. Sameshima, T. Ishikawa, H. Sumino, and N. Shinohara, "New phased array and rectenna array systems for microwave power transmission research," IEEE MTT-S International Microwave Workshop Series on Innovative Wireless Power Transmission: Technologies, Systems, and Applications, Kyoto, Japan, pp.59–62, 2011.

[7] T. Ishikawa and N. Shinohara, "Flat-topped beam forming experiment for microwave power transfer system to a vehicle roof," Wireless Power Transfer, vol.2, no.1, pp.15–21, March 2015.

[8] N. Hasegawa and N. Shinohara, "Sidelobe reduction with a GaN active array antenna," Wireless Power Transfer, vol.4, no.2, pp.113–119, Sept. 2017.

[9] B. Yang, X. Chen, J. Chu, T. Mitani, and N. Shinohara, "A 5.8-GHz Phased Array System Using Power-Variable Phase-Controlled Magnetrons for Wireless Power Transfer," IEEE Trans. Microw. Theory Tech., vol.68, no.11, pp.4951–4959, Nov. 2020.

[10] G. Pabbisetty, K. Murata, K. Taniguchi, T. Mitomo, and H. Mori, "Evaluation of Space Time Beamforming Algorithm to Realize Maintenance-Free IoT Sensors With Wireless Power Transfer System in 5.7-GHz Band," IEEE Trans. Microw. Theory Tech., vol.67, no.12, pp.5228–5234, 2019.

[11] D. Belo, D.C. Ribeiro, P. Pinho, and N.B. Carvalho, "A Selective, Tracking, and Power Adaptive Far-Field Wireless Power Transfer System," IEEE Trans. Microw. Theory Tech., vol.67, no.9, pp.3856–3866, 2019.

[12] Radiocommunication Sector of International Telecommunication Union, Recommendation ITU-R P.838-3: Specific attenuation model for rain for use in prediction methods. 2005.

[13] Radiocommunication Sector of International Telecommunication Union, Recommendation ITU-R P.530-17: Propagation data and prediction methods required for the design of terrestrial line-of-sight systems, 2017.

[14] Recommendation ITU-R P.837-7: Characteristics of precipitation for propagation modeling.

[15] H. Kazemi, "61.5% Efficiency and 3.6 kW/m^2 Power Handling Rectenna Circuit Demonstration for Radiative Millimeter Wave Wireless Power Transmission," IEEE Trans. Microw. Theory Techn., vol.70, no.1, pp.650–658, 2022.

[16] K. Ogawa, K. Ozaki, M. Yamada, and K. Honda, "High efficiency small-sized rectenna using a high-Q LC resonator for long distance WPT at 950 MHz," IEEE MTT-S Int. Microw. Symp. Dig., pp.255–258, 2012.

[17] W.C. Brown, "Electronic and mechanical improvement of the receiving terminal of a free-space microwave power transmission system," pp.51–52, 1977.

[18] A. Kumar, "Antenna assists MW power transmission," Microw. RF, vol.49, pp.70–76, 2010.

[19] X. Yang, J.-S. Xu, and D.-M. Xu, "Compact circularly polarized rectennas for microwave power transmission applications," Proc. 7th Int. Symp. Antennas Propag, EM Theory (ISAPE), pp.1–4, 2006.

[20] P. Koert and J.T. Cha, "Millimeter wave technology for space power beaming," IEEE Trans. Microw. Theory Techn., vol.40, no.6, pp.1251–1258, 1992.

[21] T. Iida, J. Pelton, and E. Ashford, Progress In Astronautics and Aeronautics: Satellite Communications In the 21st Century: Trends and Technologies, AIAA, 2003.

[22] FCC R&O (FCC 16-89), July 14, 2016 released.

[23] Y. Homma, T. Sasaki, K. Namura, F. Sameshima, T. Ishikawa, H. Sumino, and N. Shinohara, "New phased array and rectenna array systems for microwave power transmission research," IEEE MTT-S International Microwave Workshop Series on Innovative Wireless Power Transmission: Technologies, Systems, and Applications, Kyoto, Japan, pp.59–62, 2011.

[24] T. Ishikawa and N. Shinohara, "Flat-topped beam forming experiment for microwave power transfer system to a vehicle roof," Wireless Power Transfer, vol.2, no.1, pp.15–21, 2015.

[25] N. Hasegawa and N. Shinohara, "Sidelobe reduction with a GaN active array antenna," Wireless Power Transfer, vol.4, no.2, pp.113–119, 2017.

[26] B. Yang, X. Chen, J. Chu, T. Mitani, and N. Shinohara, "A 5.8-GHz Phased Array System Using Power-Variable Phase-Controlled Mag-

netrons for Wireless Power Transfer," IEEE Trans. Microw. Theory Tech., vol.68, no.11, pp.4951–4959, 2020.

[27] G. Pabbisetty, K. Murata, K. Taniguchi, T. Mitomo, and H. Mori, "Evaluation of Space Time Beamforming Algorithm to Realize Maintenance-Free IoT Sensors With Wireless Power Transfer System in 5.7-GHz Band," IEEE Trans. Microw. Theory Tech., vol.67, no.12, pp.5228–5234, 2019.

[28] D. Belo, D.C. Ribeiro, P. Pinho, and N.B. Carvalho, "A Selective, Tracking, and Power Adaptive Far-Field Wireless Power Transfer System," IEEE Trans. Microw. Theory Tech., vol.67, no.9, pp.3856–3866, 2019.

[29] B. Yang, T. Mitani, and N. Shinohara, "Evaluation of the Modulation Performance of Injection-Locked Continuous-Wave Magnetrons," IEEE Trans. Electron Devices, vol.66, no.1, pp.709–715, 2019.

[30] B. Yang, T. Mitani, and N. Shinohara, "Development of a 5.8 GHz power-variable phase-controlled magnetron," 2017 Eighteenth International Vacuum Electronics Conference (IVEC), pp.1–2, 2017.

[31] H. Huang, K. Huang, and C. Liu, "Experimental Study on the Phase Deviation of 20-kWS-Band CW Phase-Locked Magnetrons," IEEE Microw. Compon. Lett., vol.28, no.6, pp.509–511, 2018.

[32] H. Huang, L. Liu, F. Huo, Z. Liu, and C. Liu, "Microwave power combining system based on two injection-locked 15 kW CW magnetrons," 2015 IEEE MTT-S International Microwave Symposium, pp.1–3, 2015.

[33] M. Read, R.L. Ives, T. Bui, B. Chase, R. Pasquinelli, C. Walker, and J. Conant, "Advanced, phase-locked, 100 kW, 1.3 GHz magnetron," 2017 Eighteenth International Vacuum Electronics Conference (IVEC), pp.1–2, 2017.

[34] N. Hasegawa, T. Fujiwara, T. Morita, A. Kishimoto, K. Hasegawa, Y. Takagi, and Y. Ohta, "Phase-Locked Magnetrons for Beam Combining in High Power Antenna Array on MPT System," 2019 IEEE Asia-Pacific Microwave Conference (APMC), pp.905–907, 2019.

[35] N. Hasegawa, Y. Takagi, Y. Nakamoto, and Y. Ohta, "2-D Beam Steering by the Simple Phased-Array Technique for Microwave Power Transfer," 2020 IEEE Asia-Pacific Microwave Conference (APMC), pp.185–186, 2020.

Naoki Hasegawa was born in Aichi, Japan, in 1988. He received the B.E. degree in electrical and electronic engineering from Ritsumeikan University, Siga, Japan, in 2011, and the M.E. and Ph.D. (Eng.) degrees in electrical engineering from Kyoto University, Kyoto, Japan, in 2013, and 2018. Dr. Hasegawa was a Research Associate with The Japan Aerospace Exploration Agency from 2013 to 2015. His research included rf GaN power amplifier and antenna design for wireless power transfer and uplink satellite communications. He is now a system design R&D department researcher in the technology research laboratory at SoftBank Corp., Tokyo, Japan. His current research interests include rf and wireless power transfer. Dr. Hasegawa is an assistant secretary of the technical committee on IEICE microwave, a member of the international committee on IEICE wireless power transfer, and an executive chair for the 16th WPT contest of the contest committee on IEICE wireless power transfer.